Anti-Sway Control for Overhead Traveling Cranes Driven Three-Phase Induction Motor

KAMAL A. KHANDAKJI
Department of Electrical Engineering
Tafila Technical University
P.O. Box 179, Tafila 66110
JORDAN
http://www.ttu.edu.jo

Abstract: - The article proposes power semiconductor drive system, which can be used in the anti-sway control of overhead cranes driven three-phase induction motor. In this system, a current-converter has been connected to the rotor winding. Simulation of the proposed power semiconductor drive system has been developed. The mathematical model used for simulating the proposed system has been composed of standard models of the converter, three-phase slip-ring induction motor and control system. A comparison between the proposed system and the voltage-converter controlled anti-sway system has been carried out. The performance and efficiency of both anti-sway systems have been compared.

Key-Words: - Anti-sway control, overhead traveling cranes, controlled current converter, three-phase induction motor.

1 Introduction

In the last decades AC power semiconductor drives, based on different kinds of AC motors, have become the most spread electromechanical systems to generate controlled motion with high accuracy and dynamic requirements. Modern cranes are a good example of such electromechanical systems, which are equipped with ac power semiconductor drives also.

The productivity of overhead traveling cranes depends on the time required for the crane to hoist, transport and lower a load, i.e. the crane cycle time. The suspended load sway is a major problem that occurs at load transportation, increasing the total crane cycle time and thus decreasing the crane productivity in general.

The solution of such problem was and still a crucial issue for cranes designers and researchers as well [1-6].

In [7] a special control algorithm for suspended load anti-sway was developed, the developed motor torque algorithm can be realized using different power electronic circuitries. In this paper two power electronic drive systems are developed for anti-sway control and adjusted with the torque algorithm given in [7]. The first system is based on the reversible power controller (RPC), the output voltage of which is a function of the firing angle, i.e. soft starter. Therefore, the motor torque can be controlled with a special algorithm stored in the controller.

Nowadays, soft starters use special control strategies that eliminate electromagnetic torque pulsations at starting and reclosing, and keep the line current nearly constant at a preset value over the entire starting period [8].

The torque pulsation elimination strategy defines the triggering instants of the soft-starter of the supply voltages (Fig. 1).

Thyristors of the voltage controller are triggered in the sequence marked in Fig. 1, resulting in a phase difference of 60° between consecutive switchings during starting as well as in the steady state, excluding the first energization cycle. In order to eliminate supply frequency pulsations in the electromagnetic torque, different switching strategies are used for T1, T2, and T3, on the first supply voltage cycle for continuous and discontinuous line current cases, depending on whether triggering angle α is less or greater than the power factor (pf) angle of the machine at unity slip [8].

The second anti-sway electric drive system is based on a thyristor current-converter (TCC), which can be connected to the rotor winding of the slip-ring induction motor. The rotor current determines the motor torque, thus the required motor torque algorithm can be realized by creating the appropriate firing of the thyristors of the converter.

In the current paper, a try to create an anti-sway control using current converter for three-phase induction motor driven electric drives is performed.

2 Design Considerations

The block-diagram of the anti-sway electric drive system based on the RPC is shown in Fig. 2(a), a speed set point (V_{in}) is applied at the input of the control system (CS), where it is added to the negative speed feedback signal (V_{fb}), the formed error is then applied to a PID speed controller. After a signal processing at the controller stage, the output signal of the controller is applied to the firing circuit of the RPC (reversing soft starter), then the thyristors of the soft starter are triggered with a finite firing angle α, which corresponds to a finite rms value of the voltage across the soft starter. The soft starter voltage is applied to the stator winding of the 3-phase induction motor (IM).

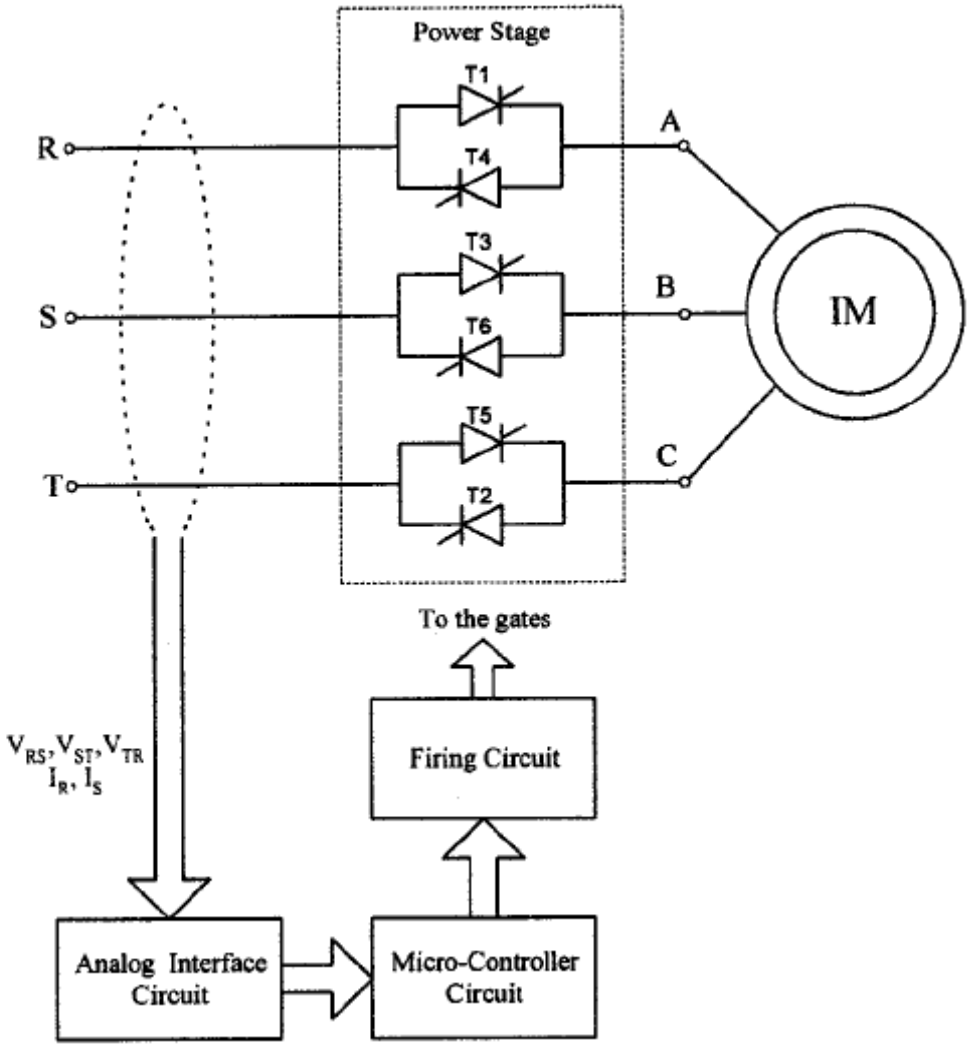

Fig.1: Schematic diagram of soft starter

The rotor winding of the 3-phase slip-ring IM is connected to external resistors R_{ext1} and R_{ext2}, this greatly increases the range of speed regulation of the system. Thus, in this system the motor torque is controlled by varying the stator voltage and the rotor resistance.

In Fig. 2(b), the block-diagram of the proposed anti-sway electric drive system is shown, a speed set point (V_{in}) is applied at the input of the control system (CS), where it is added to the negative speed feedback signal (V_{fb}), the formed error is then applied to a PID speed controller. After a signal processing at the controller stage, the output signal of the controller is applied to the firing circuit of the TCC.

The function of the current converter is to control the rotor current and thus the motor torque to achieve the required torque diagram for anti-sway control.

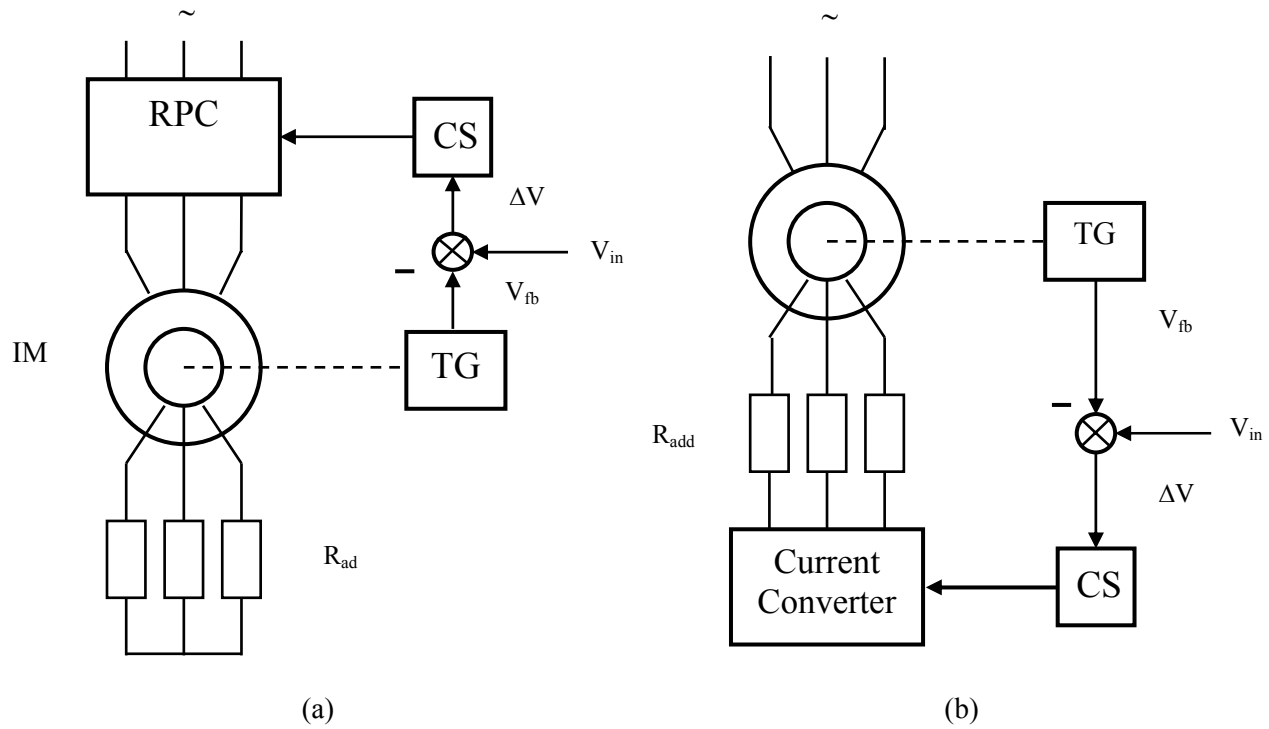

Fig. 2: Block-diagram of the anti-sway reversing power controller (a) and thyristor current controller (b) systems

3 Design and Analysis of the Power Circuit

The power circuits of the two above-mentioned systems are shown in Fig. 3. Varying the firing angle α in the RPC system, the RMS value of the voltage applied to the stator winding is also varied. This permits a torque regulation of the motor. The existence of the additional resistance in the rotor circuit R_{ad} permits a speed regulation with α = variable.

The thyristor-current converter (TCC) system permits a smooth rotor current regulation. Varying the firing angle α of thyristors T1-T3, which are connected in series with the additional resistors R_{ad1} and in parallel with R_{ad2}. If $\alpha = \alpha_{min}$ then only R_{ad1} is active in the rotor circuit and R_{ad2} is short-circuited. If the thyristors are turned off, i.e. $\alpha = \alpha_{max}$ then R_{ad2} is in series with R_{ad1}. Therefore, varying α, a family of speed-torque characteristics laying between two extreme characteristics 1- when $\alpha = \alpha$min and 2- when $\alpha = \alpha_{max}$ are formed (Fig. 4).

To minimize cargo oscillations using TCC, it is required to know the firing algorithm of thyristors T1-T3 so that the motor torque remains constant over the starting/stopping period, and the sign of the torque could be changed twice over the transient period of starting or stopping [7]. For this purpose we need to find the relationship between the motor slip (s) and the firing angle (α) so that the motor torque remains constant.

The load-phase angle of the rotor circuit can be determined as follows:

$$\varphi_r = \tan^{-1}(X_r \cdot S)/R_r \qquad (1)$$

Where X_r and R_r – the reactance and the resistance of the rotor circuit, respectively.

Varying s and using universal characteristics, we can find the value of coefficients K_r and X_r with the help of which the equivalent rotor resistance and reactance can be calculated as follows:

$$R_{eq} = R_r \cdot K_r$$
$$X_{eq} = X_r \cdot K_x \qquad (2)$$

The motor torque can be calculated using the following formula:

$$T = \frac{2 \cdot T_{max}(1 + a \cdot s_{max})}{\frac{s}{s_{max}} + \frac{s_{max}}{s} + 2 \cdot a \cdot s_{max}} \quad (3)$$

where

T_{max} – the maximum motor torque occurring at s = s_{max}

$$s_{max} \frac{R_{eq}}{\sqrt{R_1^2 + (X_1 + X_2')^2}}$$

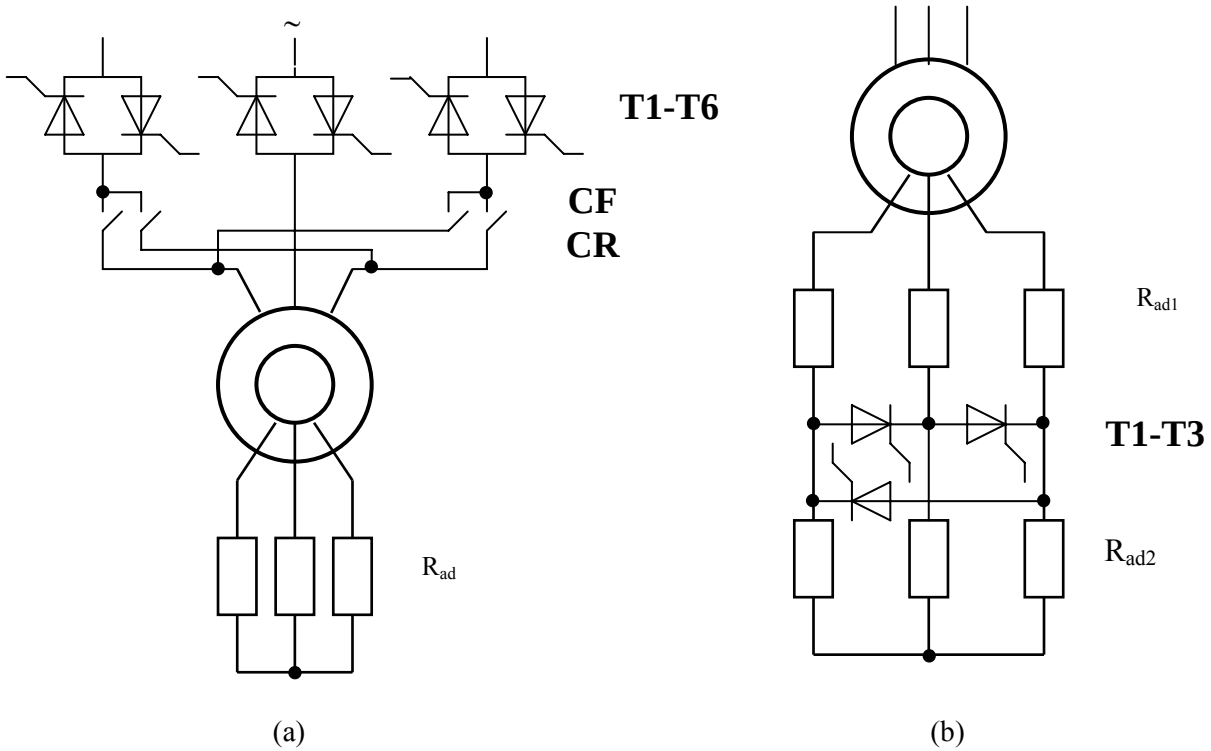

Fig. 3: The power circuits of the RPC system (a) and the TCC system (b)

Calculations were made for a real 3-phase induction motor with the following ratings:
P = 45kW, n = 576 rpm, T_{max} = 1940Nm, R_1 = 0.084Ω, R'_2 = 0.0885Ω.
The values of the additional rotor resistances are:
$R'_{ad1} = 2 \cdot R'_2 = 0.177\Omega$
$R'_{ad2} = 3.6\Omega$

The relationship α = f(s) with a motor torque = 1.2 of the nominal motor torque was calculated. With the same torque condition the stator (I_1) and rotor (I_2) currents were calculated for both systems.
The results of calculation are shown on Fig. 5 and Fig.6.
Knowing the firing algorithm α = f(s) with constant motor torque, it is possible to simulate the operation of the traveling mechanism over a full-cycle. The results of modeling are shown are shown in Fig. 7.
From Fig. 7, it is seen that the proposed thyristor current converter system can be successfully used for anti-sway control. By the end of starting, the load-sway angle α was reduced to zero, after that the suspended load was kept in a vertical position without sway over the steady-state period. At stopping, the suspended load deviates with a negative angle α, and by the end of stopping, the load was returned back to the same position with zero sway angle. The motor torque diagram was also successfully realized in accordance with the diagram derived in [7] for anti-sway control.

4 Qualitative Analysis

To make a complete comparison between both systems, calculations for the equivalent transient and steady-state stator-current (I_{1eq}) and rotor-current (I_{2eq}) for both systems have been developed.
For the full-cycle operation, the traveling distance was varied to get more information about the behavior of both systems. The results of calculations are shown in Tables 1 and 2.

Table 1: Equivalent currents of the traveling electric drive at starting and stopping

Process	**TCC**		**RPC**		t, s
	I_{1eq}, p.u.	I_{2eq}, p.u.	I_{1eq}, p.u.	I_{2eq}, p.u.	
Starting	1.67	2.14	1.29	1.75	5.5
Stopping	1.07	1.27	1.82	2.48	5.8

Table 2: Equivalent currents of the traveling electric drive for a complete cycle of operation

System	**TCC**		**RPC**		T_c, s
Traveling distance, m	I_{1eq}, p.u.	I_{2eq}, p.u.	I_{1eq}, p.u.	I_{2eq}, p.u.	
20	1.14	1.46	1.27	1.72	18.45
30	0.99	1.27	1.1	1.49	24.6
50	0.817	1.045	0.9	1.23	36.9

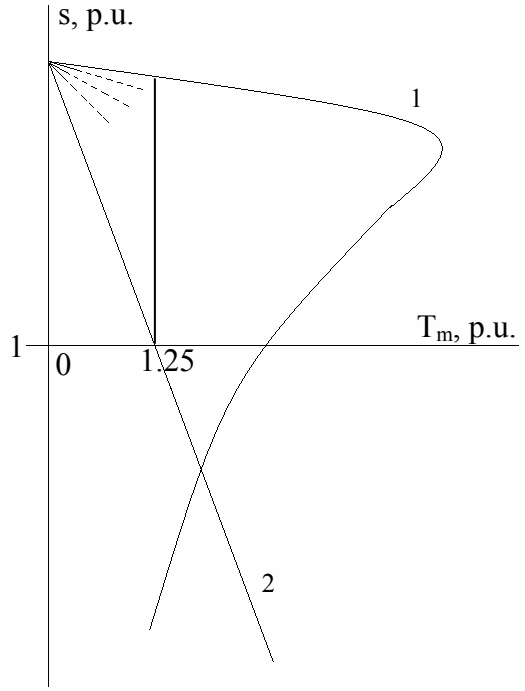

Fig. 4: Two extreme speed-torque characteristics 1 and 2

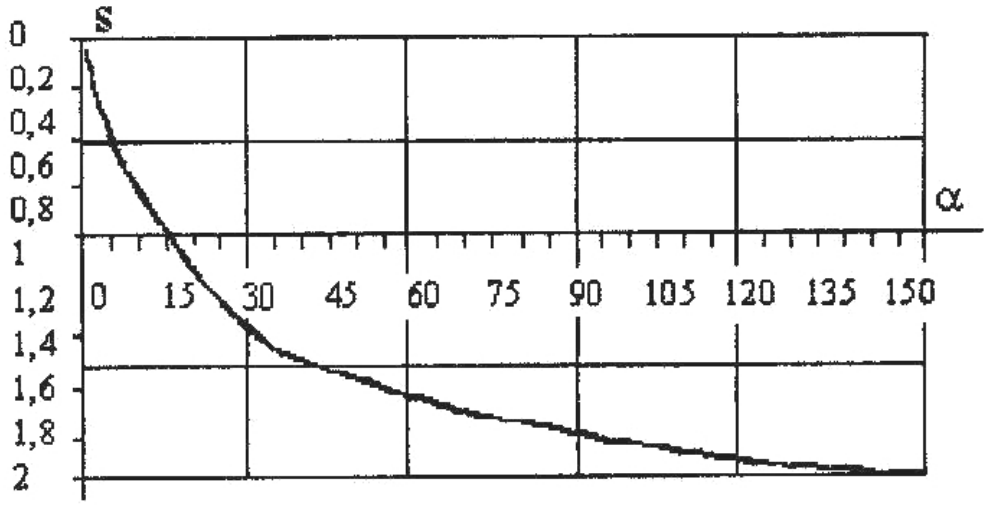

Fig. 5: The relationship between the motor-slip (s) versus the firing angle (α) with a constant motor torque = 1.25 of the rated value

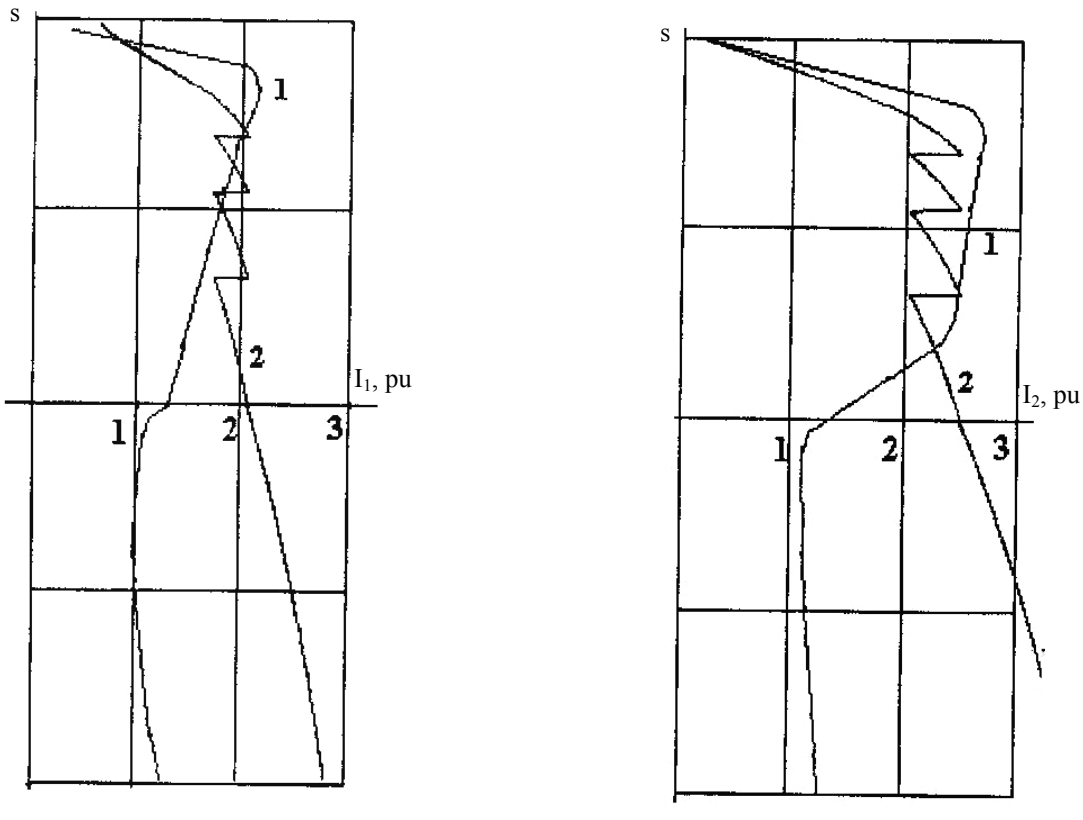

(a) (b)

Fig. 6. Motor speed versus stator-current characteristic (a) and motor speed versus rotor-current characteristic (b). 1- using TCC, 2- using RPC.

4 Conclusion

Two closed-loop power semiconductor drive systems for anti-sway control of overhead traveling cranes driven three-phase induction motor are developed. The first system controls the motor torque by changing the instantaneous voltage applied to the stator winding, while the second system controls the motor torque by changing the rotor current. Two comprehensive mathematical models for both anti-sway systems are used to

simulate the effectiveness of using the proposed systems for load anti-sway purpose in overhead cranes. The performance of the proposed systems is analyzed. Results of simulation and analysis show that both electric drive systems do eliminate suspended load sway.

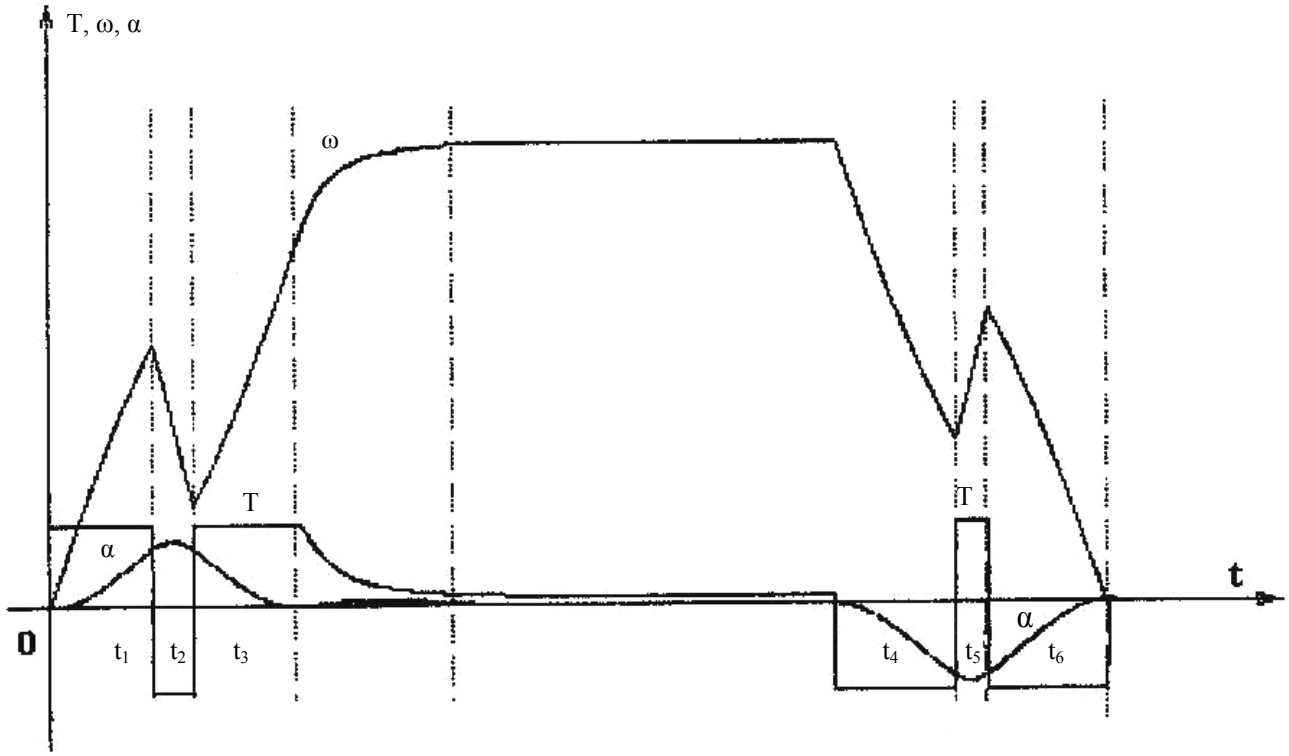

Fig. 7: Simulation results of the crane traveling electric drive for a full-cycle operation

In the TCC system, the stator equivalent current is less than the stator equivalent current in the RPC system by 10%. The rotor equivalent current (over a complete crane cycle of operation) in the TCC system is also less than the rotor equivalent current in the RPC system by 20%. Thus, it is recommended to use the TCC system.

References:

[1] Jianqiang Yi Yubazaki, N. Hirota, K. Anti-swing Fuzzy Control of Overhead Traveling Crane, *Fuzzy Systems, 2002*. IEEE Proceeding. Vol. 2, pp 1298-1303.

[2] Jung Hua Yang and Kuang Shine Yang. Adaptive Coupling Control for Overhead Crane Systems, *Mechatronics.* Elsevier. Vol. 17. Issue 2-3, March-April 2007, Pages 143-152.

[3] Yanai, N. Yamamoto, M. Mohri, A. Anti-sway Control for Wire-suspended Mechanism Based on Dynamics Compensation, *Intelligent Robots and Systems, 2002*. IEEE Proceeding. Vol. 4, pp 4287- 4292. ISBN: 0-7803-7272-7.

[4] Yanai, N. Yamamoto, M. Mohri, A. Feedback Control for Wire-suspended Mechanism with Exact Linearization, *Intelligent Robots and Systems, 2002*. IEEE Proceeding. Vol. 3, pp 2213- 2218. ISBN: 0-7803-7272-7.

[5] Yong-Seok Kim; Han-Suk Seo; Seung-Ki Sul. A New Anti-Sway Control Scheme for Trolley Crane System. *Industry Applications Conference, 2001*. IEEE Proceeding. Vol. 1, pp 548 - 552.

[6] Khandakji K.A. and Zdrozis K. Determination of Quality Parameters of Hoisting Electric Drive Systems with 3-phase Induction Motors, *Proc. 5th International Conference on Technology and Automation*, 2005. pp. 294-296.

[7] K. Khandakji. Minimization of Load Oscillations in Traveling Mechanisms of Cranes, *American Journal of Applied Sciences*. Science Publications. Vol. 2, Issue 5, 2005. pp 993-997.

[8] Gürkan Zenginobuz, Is¸ık Çadırcı. Soft Starting of Large Induction Motors at Constant Current with Minimized Starting Torque Pulsations, *IEEE Transactions on Industry Applications*, Vol. 37, Issue 5, September/October 2001, pp 1334-1347.

[9] Dewan S.B., Slemon G.R., Straughen A. Power Semiconductor Drives. *Jhon Wiley & Sons*, 1984.